Investigation of interaction of electron beam and non-linear metamaterial

PhD Thesis

Fraser Andrew Amiri-Cripps U1773291319

18th June 2019

Department of Computing and Engineering

University of Huddersfield

Contents

Chapter 1

Introduction and PhD question

Research question: Can non-linear artificial electromagnetic materials be used to mediate energy exchange between an electron beam and a wave in a novel way?

Metamaterials, or more specifically artificial electromagnetic materials, are novel man-made structures capable of exhibiting bespoke interactions with electromagnetic radiation beyond that of natural materials. Linear metamaterials have been introduced into slow wave device type electron beam systems prior to this report, but non-linear metamaterials have never been included inside any type of electron beam device. The aim of this project is to investigate a fast wave type electron beam device loaded with a non-linear metamaterial.

Chapter 2

Beam-wave Interaction Mechanisms and Metamaterials

The following sections in this chapter will provide context for the project and at the end of this chapter the various aspects presented will be tied together to discuss the project goals.

2.1   Electron beam devices

Electron beam devices in general consist of an electron gun which accelerates electrons into some type of interaction cavity where it then either interacts with an electromagnetic wave manually introduced into the system (amplifier) or, through broadband noise created by moving charged particles and resonant cavities it causes the generation of an electromagnetic field (oscillator) [1]. Initially, the focus of this project will be on amplifiers.

The set of electron beam devices operating as amplifiers can be split into two distinct subsets of systems; fast wave type devices and slow wave type devices. Slow wave type devices like the travelling wave tube or TWT principally rely on matching the axial velocity (velocity in the direction of propagation of electron beam) with the phase velocity of a wave co-propagating alongside the electrons through the device. Axial bunching of the beam by decelerating and accelerating regions of the co-propagating electromagnetic wave leads to an energy transfer between beam and wave [2]. The waves axial phase velocity is decreased from the free space velocity of light to near the velocity of the electrons in the beam via a slow wave structure. A slow wave structure can be as simple as partially loading a waveguide with a high refractive index dielectric so that the wave travels significantly more slowly than in vacuum. A slightly faster wave than electron beam results in kinetic energy being dumped into the beam and a slightly faster electron beam results in amplification of the wave [3].

The matching of the axial velocities in order for energy exchange to occur is known as the synchronicity condition for slow wave type devices. A limitation of slow wave type devices is that a slow wave structures size determines its operating frequency. Travelling wave tubes grow more difficult to fabricate as the operation frequency increases for reasons such as heating of a slow wave structure or charging of a dielectric slow wave structure in close proximity to the electron beam. These factors can adversely affect performance or prevent the system from handling particularly high powers [1]. Fast wave type devices overcome the limitations of slow wave devices by requiring different synchronicity conditions to be met

for beam-wave interaction. For example, in a gyro-travelling wave tube the synchronicity conditions require the frequency of the wave propagating in the interaction region to be close to the cyclotron frequency of an electron beam gyrating about a DC magnetic field along the axial direction. In figure 2.1 below the dispersion curve for a fast wave device can be seen. The electron beam lines from both slow and fast wave devices can be superimposed over waveguide mode curves and will intersect the curves of the modes at points where energy exchange can occur, with a slow wave beam-line represented by $\omega = v_z k_z$. The frequency, ω, at which the beam-line intersects the waveguide modes is the frequency of wave required for a given velocity of beam to interact with said wave. The fast wave beam-line is given by $\omega = v_z k_z + s\frac{\Omega}{\gamma}$ where $\frac{\Omega}{\gamma} = \frac{v_{0\perp}}{r_L} = \frac{|e|B_0}{m_0 \gamma}$. Here, r_L is the Larmor radius, or the radius from the magnetic field line and the transverse relativistic factor is $\gamma = \frac{1}{\sqrt{1-\frac{v_{0\perp}^2}{c^2}}}$, Ω is called the cyclotron frequency and the s coefficient is the sth cyclotron harmonic.

EXPLAIN CYCLOTRON HARMONICS HERE.

Although an intersection of beam and mode will indicate interaction, the ideal operating regime for fast wave devices is where the beamline grazes a waveguide mode [4].
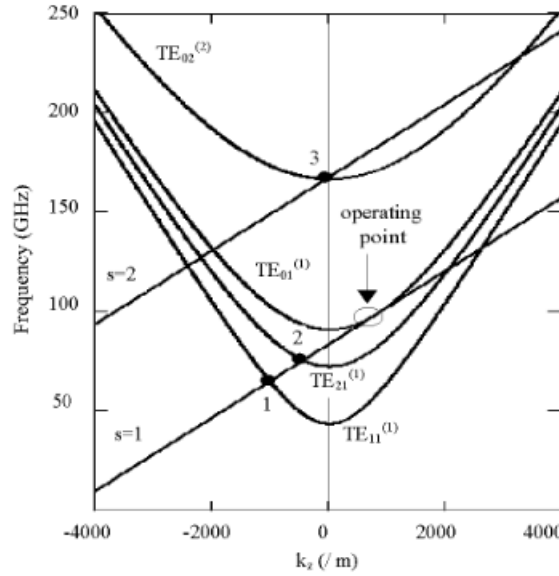

Figure 2.1: From [4]; The dispersion graph shows a fast wave interaction in a gyro travelling wave tube type device, the fast wave beam-line described by $\omega = v_z k_z + s\frac{\Omega}{\gamma}$ is superimposed on the waveguide modes for the fundamental cyclotron harmonic (s=1) and the second cyclotron harmonic (s=2).

The gyro-travelling wave tube utilises the electron cyclotron maser instability to transfer the transverse kinetic energy of electrons gyrating about the magnetic field line to the electromagnetic wave exciting the gyrating electrons [5]. As the gyrating electrons interact with the field, depending on what phase of their gyration they are in, they may lose or gain transverse velocity. If the transverse oriented electric field is slightly higher frequency than the gyro beam, then there will be a net transfer of energy to the wave,

amplifying it. As this occurs the electrons lose transverse kinetic energy and their cyclotron frequency increases, indicating the limit of energy transfer to wave is when the electrons net cyclotron frequency is higher than the waves frequency. Figure 2.2 from [1] illustrates the mechanism behind the energy transfer between beam and wave in gyro travelling wave tube when E_y electric field is directed transverse to propagation direction.
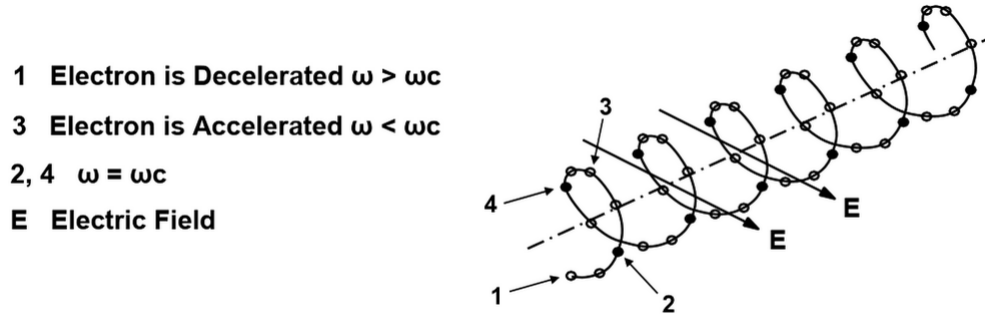

Figure 2.2: From [1]; a diagram of the physical mechanism behind electron cyclotron maser instability. Electrons travelling parallel to the E field are accelerated and their relativistic mass increases leading to a decrease in cyclotron frequency, the electrons directed anti-parallel to the E-field are decelerated leading to decrease in relativistic mass and therefore increase in cyclotron frequency. The electrons perpendicular to E-field are unaffected.

An electric field directed transverse to the propagation direction of the electron beam will cause orbital bunching to occur. This orbital bunching is a relativistic effect driven by the change in mass. A gyrotron device is composed of a magnetron injection gun (a cathode with a nearly axial magnetic field and nearly radial electric field leading to cycloid orbits of electrons emitted and which produces an annular distribution of electrons [1]), the interaction circuit (which can just simply be a waveguide cavity), a collector (which the beam is deposited onto at the end and can simply be a conical cavity with a diameter that increases in the propagation direction), an RF output window (and RF input in the case of gyro-TWT) and finally a solenoid surrounding the device to provide the axial DC magnetic field line about which the electrons gyrate. See figure 2.3 below for clarification of the set up of a gyro-monotron (oscillator) the amplifier version of the device (gyro-TWT) simply has an additional RF input.
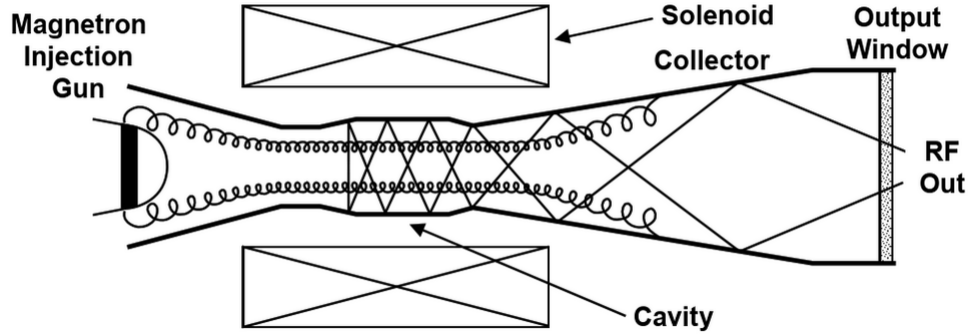
Figure 2.3: From [1]; A diagram of a basic gyrotron set up.

To summarise, a fast wave device is a device in which an electron beam interacts with the waves in a waveguide without the waves having to be slowed down. A travelling wave tube is a slow wave amplifier device, whereas a gyro-travelling wave tube is a fast wave amplifier device. The focus of this project was originally investigating sub wavelength periodic structures called non-linear metamaterials and their ability to act as slow wave structures, but as the available laboratory equipment requires the metamaterial to be resonant in X-band (8-12GHz), it proved exceptionally difficult to design a non-linear metamaterial that matched this criteria whilst also operating as a slow wave structure. Instead, a fast wave device was chosen for loading with non-linear metamaterial.

2.2 Metamaterials

Metamaterials are defined by Rodger Walser as "...macroscopic composites having a man-made, three-dimensional, periodic cellular architecture designed to produce an optimized combination, not available in nature, of two or more responses to specific excitation"[6]. For example, metamaterials are capable of exhibiting simultaneously negative permittivity and permeability leading to a negative refractive index, a phenomena not found in nature. A metamaterials interaction with incident electromagnetic radiation is dependent on its geometry, leading to tailor-able media that can be designed to meet specific requirements. The type of unit cell which has been chosen for this project is the simplest and most well documented; the single split ring resonator. The single split ring resonator or SRR is a metallic (usually copper) ring on top of a dielectric substrate. This metamaterial can be fabricated through printed circuit board methods aslong as the feature size does not require a resolution more precise than 0.05mm due to several PCB services stating this as their minimum resolution.

The ring has a split cut out of it leading to a capacitive effect which allows the meta-atom or unit cell to be modelled as an LRC series circuit (capacitance from split, resistance from resistivity of copper and inductance from the mutual inductance between neighbouring excited rings in a periodic array).

Similar to an LRC circuit, the meta-atom will exhibit resonant behaviour in response to an

incident wave around the structures resonant frequency. To excite an SRR, a electromagnetic field can be imposed upon the structure, with the magnetic component directed through the centre of the ring, then according to Faraday's law a circulating current will be induced. The circulating current through the ring will create a potential difference across the capacitive split gap and hence strongly localise the electric field in the split around resonance. This localised field is analogous to a dipole in a natural material. Effective media theory states that provided the meta-atom unit cell is sufficiently sub wavelength (d $\sim \frac{\lambda}{10}$) where d is unit cell size (width and height of substrate underneath ring), the wave will interact with a periodic array of unit cells as if the periodic array of unit cells is a continuous material. From this material, or metamaterial, effective constitutive parameters can be obtained from standard retrieval procedures such as the Nicholson-Ross-Weir method discussed in chapter... Parameters such as refractive index, permittivity and permeability can be evaluated using a simulation or experiment to obtain scattering parameters and then through a custom code based off of the Smith adaptation of the Nicholson-Ross-Weir approach (adapted to allow negative refractive index materials)

, the scattering parameters can be used to calculate the constitutive parameters of the metamaterial.

2.3   Non-linearity in metamaterials

To enable the metamaterial to exhibit a non-linear response a non-linear dependence on the incident wave must be somehow incorporated. Treating the unit cell as an LRC circuit instantly indicates that a non-linearity could appear in the inductance, capacitance or resistance of the system to generate the desired response. A varistor or variable resistor could theoretically introduce this non-linearity, but as the split ring resonator is the geometry of choice due to its simplicity, the varistor would not work. If a second split gap was introduced opposite to the initial gap, and included a varistor in series with the second gap, this might achieve the desired effect, however, with the single split ring resonator the varistor can not be placed across the split ring gap as it would remove the capacitive effect and the meta-atom would no longer be resonant. The inductance is related to the coupling of adjacent meta-atoms so introducing a piezo-electric substrate for which the inverse piezo-electric effect (electrostriction) could be exploited at a region on the E-field vs strain plane that demonstrates a non-linear relationship, could lead to a mechanical strain type non-linearity in the inductance due to a non-linear variation of inter-cell distances with applied field. This however would be impossible to model with the software available in a reasonable time. Finally, the remaining choice, non-linear capacitance, leads to the more commonly used methods for fabricating non-linear metamaterials. Non-linear capacitance can be achieved via the inclusion of a varactor or variable capacitance diode, or alternatively via thin film Barium Strontium Titanate or other (NONLINEAR CRYSTALS?). Barium Strontium Titanate thin film would be difficult to model with the available software so a diode with a capacitance that depends non-linearly on the voltage applied across it was chosen as circuit SPICE models are readily available for diodes which aid simulation.

The non-linear response to incident radiation in general is a result of at least one non-zero second order or higher electric or magnetic susceptibility present in the material. In the case of natural materials it is usually the electric susceptibility which is the dominant factor

causing a non-linear response.

Maxwells equations describe the displacement field in a system with a non-linear response to an electric field as:

$$\vec{D} = \epsilon\vec{E} + \vec{P}^{NL} \tag{2.1}$$

Where ϵ is the permittivity $= \epsilon_0(1+\chi^{(1)})$ and $\vec{P}^{NL}$ is the series of higher order susceptibilities:

$$\vec{P}^{NL} = \epsilon_0(\chi^{(2)}\vec{E}\vec{E} + \sum_{i=3}^{\infty}\chi^{(i)}\vec{E}^i) \tag{2.2}$$

Deriving the wave equation in a region with no charges via the standard Helmholtz procedure of taking the curl of the curl of E, substituting in relevant Maxwells equations and using appropriate vector calculus identities leads to:

$$\nabla^2 E - \mu_0\epsilon\frac{\partial^2\vec{E}}{\partial t^2} = \mu_0\frac{\partial^2\vec{P}^{NL}}{\partial t^2} \tag{2.3}$$

This wave equation is driven on the right hand side by the non-linear polarisation terms, this can be compared to a linear material which has no non-linear polarisation and hence has a zero on the right hand side. Assuming the E field is in the form of a plane wave propagating in the Z direction ($E_0e^{i(\omega t - k_z z)}$) and assuming that the incident wave is not very intense or an ultra short pulse which varies rapidly over one wave cycle the slowly varying envelope approximation can be employed. The slowly varying envelope approximation assumes some function A(z,t) varies slowly in terms of z and t such that the second and higher order derivatives can be considered negligible in comparison to first order derivatives.

Imposing waves on the material will lead to a phenomena called wave mixing discussed in subsection 2.3.1 below. Using the slowly varying envelope approximation and subbing the different fields imposed on the material into equation 2.3 and after some lengthy algebra (detailed in progression monitoring one) relations describing the flow of energy in non-linear media between coupled harmonics and a fundamental wave known as the coupled wave relations can be obtained, which in the case of both waves imposed having identical frequency (second harmonic generation) the relationship is:

$$\frac{\partial E_1}{\partial z} = \frac{-i\omega_1}{2cn_1}\chi^{(2)}E_2E_1^*e^{-i\Delta kz}$$

$$\frac{\partial E_2}{\partial z} = \frac{-i\omega_2}{4cn_2}\chi^{(2)}E_1^2e^{i\Delta kz} \tag{2.4}$$

Where E_1, E_2 are the amplitudes of the wave at frequency ω_1, ω_2 respectively, n_1, n_2 are the refractive indices at the two frequencies involved in second harmonic generation, $\chi^{(2)}$ is the second order susceptibility responsible for the second harmonic generation (or SHG) and Δk is a parameter called the phase mismatch parameter. The phase mismatch for a given non-linear process describes the phase relationship between interacting waves as they propagate through a specific material. If phase mismatch is not close to zero for a particular spectral component of the polarisation or magnetisation in a material, then the spectral component

will be negligible due to destructive interference by the time it reaches the exit boundary of the material. Usually only one spectral combination will be well phase matched, so only one wave mixing process will need to be considered if several incident waves are present.

In the case of non-linear metamaterials and for the particular non-linear process of second harmonic generation which is the simplest wave mixing process because $k_{fundamental} = k_{other-incident}$, the phase mismatch parameter can be defined as:

$$\Delta k = k_{resultant} - (k_{fundamental} + k_{other-incident}) = k_2 - 2k_1 = 2\omega_1(\frac{n_2 - n_1}{c}) \qquad (2.5)$$

Where n_1, n_2 are the refractive indices of the metamaterial at frequency 1 and frequency 2 respectively (fundamental frequency and second harmonic in the case of second harmonic generation). The phase matching parameter becomes necessary in the presence of a chromatically dispersive medium, or in other words a medium of which the refractive index depends upon frequency of incident wave.

2.3.1   Wave mixing

Wave mixing is a well known non-linear phenomena in which incident waves can couple via the susceptibility of a material to generate a wave with a different frequency. The two incident frequencies can be the same, as is the case with second harmonic generation where two waves of frequency ω couple to produce a wave of frequency 2ω. The quantum mechanical picture of this process is two photons of the initial frequency are up converted to one photon of the second sum frequency. Three wave mixing occurs with second order susceptibilities as can be seen from equation 2.2, where two fields are produced with the second order susceptibility which will generate a new field. In three wave mixing two waves couple via a second order susceptibility and the result will be a third wave. The identity of these constituent waves can be understood from commonly used indices on the susceptibility (which were suppressed in 2.2 above for brevity). The indices used for defining the magnetic susceptibility coupling two magnetic fields to create a third magnetic field is $\chi^{(2)}_{mmm}(\omega_l; \omega_n, \omega_o)$, where the subscript "mmm" refers to the three waves in the mixing process, the first m is the type of field resulting from the coupling (e for electric, m for magnetic), the second and third m reveal the two fields involved in the coupling process. In the argument of the susceptibility the three frequencies can be seen, the first frequency is the frequency of the resultant wave, the second and third the frequency of the coupled waves. To fully describe a material, a susceptibility tensor is needed, which includes more indices $\chi^{(2)}_{mmm,yyy}(\omega_l; \omega_n, \omega_o)$, the new subscript refers to the direction each wave in the mixing process is polarised in. In the simulations performed for this report, the susceptibility tensor element being probed is $\chi^{(2)}_{mmm,yyy}(\omega_l; \omega_n, \omega_o)$, where the magnetic fields incident on the structure for coupling will be directed into the centre of the ring and any resultant magnetic wave harmonics will be directed the same way. Electric fields will naturally be created as well, but as the second order magnetic susceptibility of interest is known to be the dominant coupling term for this geometry, harmonics resulting from other coupling terms will be negligible.

Besides the wave mixing processes that result in the generation of harmonics, there is another factor to consider with respect to the interaction of a non-linear material and electromagnetic radiation. As the incident radiation power increases, the resonance frequency of the

metamaterial will change. In the case of the metamaterial under study, the resonance frequency decreases with increased power. It is vital to consider how this tuning will affect the constitutive parameters of the metamaterial, as it could mean a small increase in the amplitude of the incident wave leads to the metamaterial loaded waveguide behaving completely differently. The method for calculating the resonance tuning will be discussed in chapter METHODOLOY CHAP HERE.

2.4 Project goals

The goal and novelty of this project involves investigating non-linear metamaterials in a gyro-travelling wave tube type device. Before proceeding with experiments the tuning of the metamaterial must be evaluated so that the effect of the electron beam amplifying the wave can be included in the considerations concerning experimental equipment. The tuning will reveal how the basic dispersion relation is effected by an increase in power and will dictate the choice of input signal frequency as well as the strength of the DC magnetic field about which the electrons will gyrate. The results in this report revolve around this step. After some initial cold testing has been performed and the gain through the device has been found experimentally for a small signal over a small propagation distance (VERIFY WHAT DISTANCE WUT WUT WUT), the harmonics created will be predictable through the coupled wave equations above upon assuming the non-depleted pump approximation. DISCUSS NDP AND RELATIONSHIP TO COUPLED WAVE EQUATIONS. Once the coupled wave equations are evaluated, the next step of the project can begin; ascertaining whether a cyclotron harmonic at an eigenfrequency of the interaction cavity can couple with an input signal to generate a third wave via a novel example of three wave mixing. Once this has been explored, the final and most interesting step will be to investigate whether or not cyclotron harmonics can through broadband noise and with the gyro device acting as an oscillator, generate a signal in the cavity, and then if that signal alone or a combination of generated signals can be used in another novel three wave mixing process that would involve no input signal. If both processes are found to be achievable experimentally, this work could have huge ramifications for the terahertz gap problem, which is a region around 1THz which is infamously difficult to efficiently produce radiation in. The reason for the ramifications, is that due to Maxwells equations being scale invariant, isotropic downscaling of the device could lead to a system that instead of operating around X-band, operates in exactly the same manner around the millimetre wave regime (100's of GHz) and harmonics produced via the novel three wave mixing discussed above could provide a viable alternative route to producing radiation in the region of the electromagnetic spectrum described as the terahertz gap.

Chapter 3

Methodology

To expedite the process of moving from theory and simulation to laboratory experiment, the specific experimental set up required will be found by characterising the interaction of electromagnetic wave and non-linear metamaterial, then using this characterisation to predict specific experimental parameters such as dimensions of waveguide, accelerating potential of electron gun, frequency of input signal and strength of DC magnetic field required.

Firstly, the Smith adaptation of the Nicholson-Ross-Weir method will be used to characterise the constitutive parameters of the metamaterial. The Nicholson-Ross-Weir method will provide: permittivity, permeabiliity, refractive index, impedance as well the resonance frequency. After finding these parameters for the linear meta atom, which refers to the low voltage regime of the meta atom with varactor inclusion, the elements of the susceptibility tensor pertaining to the specific polarisations of incident waves we are interested in can be found.

The Smith adaptation of the Nicholson-Ross-Weir method takes into account the possibility of negative refractive index with metamaterials. COMSOL$^{(tm)}$ will be used to find the scattering matrix components of the metamaterial under study. COMSOL$^{(tm)}$ is a software which functions as a PDE solver, with a visual graphics user interface, allowing an intuitive set up of complicated physical systems and numerically calculates solutions to PDE's that describe physical phenomena using finite element method. This means it separates a model into discrete subdomains, in each subdomain it numerically solves the relevant maxwell equations to find the electric/magnetic field or other quantity expressed by an equation at this spatial point for a given frequency or time. We can then export the calculated S11 and S21 parameters to MATLAB$^{(tm)}$ to calculate the following using my NRW/Smith adaptation code:

$$Z = \pm \left[\frac{(1 + S_{11})^2 - S_{21}^2}{(1 - S_{11})^2 - S_{21}^2} \right]^{\frac{1}{2}} \tag{3.1}$$

$$\Re(n) = \pm \frac{1}{kd} \Re \left[\arccos(\frac{1 - S_{11}^2 + S_{21}^2}{2 S_{21}}) \right] + \frac{2\pi m}{kd} \tag{3.2}$$

$$\Im(n) = \pm \frac{1}{kd} \Im \left[\arccos(\frac{1 - S_{11}^2 + S_{21}^2}{2 S_{21}}) \right] \tag{3.3}$$

Where effective permittivity and effective permeability (from effective media theory) $\epsilon_f = \dfrac{n(\omega)}{Z(\omega)}$ and $\mu_f = n(\omega)Z(\omega)$. In the above equations, m is an integer, k $= \dfrac{2\pi}{\lambda_0}$ is the free space wave vector, d is the unit cell size and Z, n, ϵ_f and μ_f are complex valued parameters. The real part of Z is the resistance, and the imaginary part is the reactance. Reactance is a circuit element's opposition to change in current (voltage) due to inductance (capacitance). The real part of ϵ_f is a measure of the resistance to forming an electric field in a particular effective medium. The imaginary part of ϵ_f is related to losses due to relaxation of dipoles and energy lost due to electrical energy being stored in a resonance. The real part of μ_f is a measure of how easily a magnetic field can 'permeate' an effective material. The imaginary component of μ_f arises from the phase lag between the magnetic field and the magnetization of the effective media, it relates to losses in the material due to magnetic dipole relaxation and energy lost in resonance. The real part of the refractive index relates to the change of velocity of EM radiation at the boundary between free space and the media in question. The imaginary part of n relates to the attenuation of the wave in a medium.

To simulate the non-linear metamaterial, the linear regime (very low voltage across diode) of the non-linear metamaterial was examined. Using circuit physics in COMSOL$^{(tm)}$ and the MLC representation of a variable capacitance diode , it was possible to simulate the meta-atom and diode system by approximating the diode as a linear capacitor with a capacitance that is identical to the junction capacitance provided in datasheets pertaining to a particular diode. The packaging inductance and series resistance was also included, which meant the simulation would take into account self resonance (as the diode mimicking circuit is now also itself an LRC circuit). Many diodes were tested this way, but as the metamaterial is required to be resonant in X-band (8-12GHz), it was found that a very low junction capacitance diode was necessary. Given the fact that placing the diode across the split gap modified the LRC properties of the split ring as the diode will act in parallel with the capacitance of the split gap, meaning that the new total capacitance of the SRR-diode system is the sum of the capacitance of the original split ring and the capacitance of the diode. As resonance frequency is described by $\omega = \frac{1}{\sqrt{LC}}$ in an LRC circuit, this means the lower the capacitance of the system the higher the resonance. Due to the requirement of having to manually attach the diodes to the metamaterial after the linear metamaterial has been fabricated via PCB methods by an outside company, the unit cell needed to be as big as possible. Around 5mm unit cell size the junction capacitance of the diode inclusion needed to bring the resonance of the metamaterial up to X-band was found to be around 0.06pF by trial and error testing.

[35].

However, phase matching conditions mean that generally speaking only one spectral component of the magnetisation term will propagate through the material as the other components destructively interfere with newly produced magnetisation components throughout the media. For now phase matching will be left as natural, so as to focus other properties. By natural phase matching it is meant that no phase mismatch reduction techniques will be used, and only the naturally occurring phase matching of the metamaterial will be used. Before this step though the first aspect of the non-linearity that needs to be investigated is the tuning. In order to evaluate this property the method outlined by Poutrina in [33] will be used.

In this paper the author discusses the characterisation of metamaterial with similar ge-

ometry to the meta atom chosen for this project.

Poutrina simulates the linear regime of the NL metamaterial on COMSOL which she then exports the S parameters into a custom matlab code. This allows a Nicholson-Ross-Weir routine to evaluate the constitutive parameters. The permeability of the metamaterial is then curve fitted to an equation representing a Lorentzian oscillator. This allows the free parameters, resonant frequency, non-linear oscillator strength F and loss Gamma to be found. Once these parameters are found, they can be used in a non-linear differential equation to self-consistently find the voltage across the split gap and the capacitance that results from the SPICE model parameters of a chosen diode for a given frequency and amplitude of incident H field. Upon solving this ODE by setting up MATLAB's built in Runge-Kutta ODE45 solver, the solution for the equation in terms of q can be found over a range of time for a given frequency and amplitude of incident H field. The results can then be fourier transformed to the frequency domain and then the harmonics can be averaged as outlined in the Poutrina method. This process can be repeated for a range of incident frequencies for a given amplitude. This process can be repeated for each given amplitude and eventually the capacitances dependence on applied voltage and frequency can be found and utilised as a lookup table in COMSOL$^{(tm)}$ to model the resonance tuning and obtain S-parameters. These new S-parameters can be used to evaluate how the constitutive parameters vary with tuning. With this knowledge the dimensions of the waveguide can be chosen so that the interaction with the electron beam is with the fundamental mode in the waveguide at a frequency between 2-12GHz as per Professor Seviours given specifications.

To find the intersection of beam and wave a dispersion model can be used that treats the system as a fully metamaterial filled waveguide through which an electron beam will propagate. A fully filled waveguide seems counter-intuitive as there will need to be a vacuum gap in the centre for the electron beam to propagate, however, a metamaterial unit cell has a considerable amount of empty space. The unit cell is a cube, and includes air or vacuum gap between adjacent unit cells SEE IMAGE BELOW. This gap between unit cells can be utilised for the electron beam passage.

It has been demonstrated with a linear dielectric (not metamaterial) in a gyro travelling wave tube that lining tube with dielectric can widen the frequency band over which an interaction can occur [59], it would be interesting to see if this same effect can be witnessed with metamaterials experimentally, it would also be interesting to see if this effect is increased by the tuning. This is another potential avenue of investigation that may be eventually explored experimentally and another reason that knowledge of how the tuning affects the parameters is paramount. This will be considered further in future work.

To find the best metamaterial unit cell for the experimental phase, many different metamaterials were initially considered, including metamaterials that exhibit negative refractive index. Eventually however, the choice of geometry was dictated by the metamaterial easiest to add non-linearity too. The single split ring resonator was chosen due to its simplicity and the fact that its behaviour is well documented, including its behaviour with a variable capacitance diode inclusion, leading to confidence in the parameter retrieval techniques as it was possible to reproduce other authors results then move onto producing the results in this report. In terms of desirable linear regime of non-linear metamaterial parameters, there are several factors at play such the sign of the real parts of permeability and permittivity at the chosen frequency, for example, ϵ and μ either both need to be positive or both negative for

wave propagation[23].

In terms of non-linear beam wave interaction, to reduce reflection in the system as a result of the metamaterial constitutive parameters changing because of a tuning the impedance of a non-linear material in the wave amplifying electron beam device will have to gradually change with resonance tuning [64]. In turn this implies that the impedance of the linear regime of the non-linear metamaterial will need to change slowly with frequency, in the neighbourhood of the desired frequency for interaction.

Provided the above conditions are met, the metamaterial should provide a good candidate for the investigation of interaction of electron beam and wave in a non-linear metamaterial. The following meta atom in figure 3.1 was chosen which meets all the above requirements when an incident field is oriented with magnetic field through centre of ring.

Figure 3.1: 3mm unit cell split ring resonator meta atom chosen for investigation.

The constitutive parameters seen below in figures 3.2(a), 3.2(b), 3.2(c) and 3.2(d) meet the gradual impedance change, refractive index near zero and double positive μ, ϵ conditions above.

(a) (b)
Real impedance
fraction
tive in-
linear
index regime
of meta-
limitaia-
eattre-
regiahe
metho-
masen.
te-
rial
cho-
sen.

(c) (d)
Reer-
mmite-
tiabil-
itiyy
ooff
lilima-
eaatr
reggiunee
mmeetha-
mmaa-
ttee-
riiadl
chloe-
sseen.

Figure 3.2: Linear metamaterial constitutive parameters retrieved via COMSOL$^{(tm)}$ simulation of coupled circuit and wave physics followed by MATLAB$^{(tm)}$ analysis of S parameters.

Off resonance the metamaterial is not very dispersive so the parameters are almost constant over 7-10GHz. To verify the accuracy of the results of the COMSOL$^{(tm)}$ to MATLAB$^{(tm)}$ pipeline, results from other papers characterising linear and non-linear meta-atoms were reproduced and these reproductions can be found in the verification section of the appendix.

Eventually, after evaluating the gain due to tuning experimentally, the next step will be to consider the coupling of an input signal and cyclotron harmonic exciting an eigenfrequency of the cavity. The eigenfrequency of the loaded interaction cavity will be found via an eigenfrequency study on COMSOL$^{(tm)}$. The coupled wave equations can then be used, once the phase mismatch parameter has been computed for a given wave mixing process. In order to calculate the second order susceptibility for a given wave mixing process a method outlined by Poutrina et al can be used:

$$\chi_m^{(1)}(\omega_n) = \frac{N\omega_0^2\omega_n^2A^2\mu_0C_0}{D(\omega_n)} \tag{3.4}$$

$$\chi_m^{(2)}(\omega_l; \omega_n, \omega_m) = \frac{-ia\omega_0^6(\omega_n + \omega_m)\omega_m\mu_0^2A^3NC_0}{D(\omega_n)D(\omega_m)D(\omega_n + \omega_m)} \tag{3.5}$$

Where D is a resonance denominator and is $D(\omega_n) = \omega_0^2 - \omega_n^2 - i\gamma\omega_n$, where γ is related to loss. The parameters above are; $N = \frac{1}{d^3}$ where d is the unit cell size, ω_0 is the linear resonance frequency, ω_n, ω_m, ω_l are three frequencies of wave involved in a mixing process caused by coupling of ω_n, ω_m via the second order susceptibility. $\omega_l = \omega_n + \omega_m$. C_0 is the junction capacitance of the variable capacitance diode, A is the area of the split ring and "a" is a non-linear co-efficient found by Taylor expanding the exact expression of non-linear capacitance, see [33] for more details. In the general geometry of unit cell case, to retrieve the non-linear susceptibilities the non-linear transfer matrix approach would have to be utilised, [60]. However, for the simple case of a single split ring resonator, Poutrina's equations can be used.

(a) (b)
First Sec-
order ond
χ ob- or-
tained der
via χ
Point- ob-
ing tained
via
equa-
tions
for
sin-
gle
fre-
quency
in-
ci-
dent
field

(c)
Res-
o-
nance
tun-
ing
over
a
range
of
pow-
ers.

Figure 3.3: non-linear characterisation of metamaterial for single frequency incident field, a) first order susceptibility, b) second order susceptibility, c) Resonance tuning from ODE45 and Fourier transform method.

Chapter 4

Results and Guidance for Experimental Set Up

Chapter 5

Cold Testing, Fabrication and other Preparations

Chapter 6

Future Work

This section will reference the attached Gantt Chart. Work package 1 is a source collection phase and will continue over the course of the next few months, however it will be a small task done once or twice a week over this period. Work package 2 will involve several detailed phases. W.P. 2.1 will begin by re-deriving the dispersion relation for the gyro travelling wave tube but this time including several novel factors. The first novel factor is the harmonics generated by the non-linear metamaterial in the waveguide. The effect on the distribution of the electrons in the electron beam would be taken into account before utilising the linearised Maxwell-Vlasov equations. The resonance tuning will be calculated via COMSOL$^{(tm)}$ so that as the wave is amplified by the beam in the device the new material properties can be found so a changing dispersion relation can be plotted. This may lead to an improvement on beam-wave interaction which would mean a more efficient gyro travelling wave tube than that of a conventional set up. At this point, the penultimate theoretical investigation would be the case of a cyclotron harmonic exciting an eigenmode of the waveguide above the frequency of the input signal and therefore acting as the pump for a three wave mixing process such as sum frequency, difference frequency or non-degenerate parametric amplification. The final theoretical investigation before optimisation and fabrication can begin is to investigate if the gyrotron can be made to operate as an oscillator and if it could interact with the non-linear metamaterial in such a way, that the cyclotron harmonics could act as signal and pump and then generate an idler wave in the metamaterial and invoke a non-linear response in the media to trigger a three wave mixing process. All without the need for an external signal to be introduced into the waveguide.

W.P. 2.2 Will happen simultaneously with W.P. 2.1) and will involve incorporating the non-linear beam dynamics into the model. This will be approached analytically but solved numerically. W.P. 2.3) will only be undertaken if time permits, and involves creating a theoretical model for a non-linear metamaterial acting as a slow wave structure. If the theory is completed, a theoretical paper may be published.

W.P. 3 involves expanding the computational skills gained up to this point and also exploring the possibility of using particle in a cell software MAGIC from Orbital ATK to simulate the non-linear metamaterial in a rectangular wave guide in proximity to a gyrating electron beam. MAGIC may not be capable of simulating the non-linear metamaterial though, so this step may be disregarded at a later date. W.P. 3.2 concerns the symbolic tools available within MATLAB$^{(tm)}$ as the dispersion relation for the gyro travelling wave tube will likely

involve an incredibly complicated algebraic expression which will require a lot of time to solve by hand but could be vastly sped up if the symbolic tools can lighten the load.

W.P. 4.1 involves using MAGIC to simulate the system, this step requires the knowledge of whether or not MAGIC is capable of doing so, but also how to use MAGIC to do so. W.P. 4.2 will be used in conjuction with the symbolic tools, ODE solvers and other numerical techniques will be used to tackle the model once non-linear beam dynamics have been incorporated.

W.P. 5 Has been alotted several months as the author of this report has a theoretical physics background and expects a steep learning curve for the experimental techniques and statistical data analysis methods. W.P. 6 will begin as soon as the previous work package can be considered complete, which may be slightly sooner than the alotted time. W.P. 6.1 and 6.2 will be simple experiments should take no longer than several weeks to complete. W.P. 6.4 will be the major chunk of experimental work for the thesis. W.P. 6.5 will only take place if time permits and the pre-requisite theoretical model for slow wave structures has been completed. W.P. 7 and 8 will sporadically throughout the next 15 months, with the focus shifting solely onto these two packages over the last 3 months before thesis submission.

Chapter 7

Conclusion

The project has begun to gain momentum, and the work so far has been encapsulated by the preceeding report. The initial idea to investigate a novel slow wave device has been ruled out by the necessity of an extremely low junction capacitance varactor. A fast wave device relying on the electron cyclotron maser instability and interaction with a non-linear metamaterial loaded waveguide modes has become the object of interest. Investigation of the non-linear effects have started with the study of the gyro travelling wave tube amplification leading to resonance tuning of the non-linear metamaterial and consequently changes in the material parameters and dispersion relation. The future work summarised in the previous section will begin shortly and the author expects to finish the theoretical work in three months or less so that there is plenty of time to undertake experimental work to verify the numerics and the theory.

Chapter 8

Thesis foundation

CPML, PLRC, nonlinearity in PLRC

FULL MAXWELL EQUATIONS FOR NONLINEAR DISPERSIVE CASE MULTIPLE
POLES SUMMATION!!!! TESTS: TRANSMISSION AND REFLECTION ANALYSIS

Pertinent Maxwell Equations: Below the coupled maxwells equations describing displacement field and magnetising field (B) are provided, a star operation indicates a convolution in the time domain or a multiplication in the frequency domain.

$$\nabla \times H(t) = \frac{\partial D}{\partial t} + \sigma_E \star E(t) \tag{8.1}$$

$$\nabla \times E(t) = -\frac{\partial B}{\partial t} + \sigma_M \star E(t) \tag{8.2}$$

Where D is:

$$D(t) = \epsilon_0 \epsilon_\infty E(t) + \epsilon_0 \sum_{i=0}^{q-1} \int_{i\Delta t}^{(i+1)\Delta t} E(t-\tau) \chi_E^{(1)}(\tau) d\tau \tag{8.3}$$

And B is:

$$B(t) = \mu_0 \mu_\infty H(t) + \mu_0 \sum_{i=0}^{q-1} \int_{i\Delta t}^{(i+1)\Delta t} H(t-\tau) \chi_M^{(1)}(\tau) d\tau \tag{8.4}$$

$$+\mu_0 \sum_{i=0}^{q-1} \int_{i\Delta t}^{(i+1)\Delta t} \int_{i\Delta t}^{(i+1)\Delta t} H(t-\tau) H(t-t_1) \chi_M^{(2)}(\tau, t_1) d\tau dt_1$$

Assuming conductivities can be treated as linear entities, magnetic 'conductivity' (or loss from permeance):

$$\sigma_E(\omega) = (\epsilon(\omega) - \epsilon_0) j\omega \tag{8.5}$$

And loss from electric field interaction is:

$$\sigma_M(\omega) = (\mu(\omega) - \mu_0) j\omega \tag{8.6}$$

The time domain convolution of the dispersive conductivities and the relevant field quantities are as follows with the magnetic loss and H field:

$$\Sigma_E(t) = \epsilon_0 \sum_{i=0}^{q-1} \int_{i\Delta t}^{(i+1)\Delta t} E(t-\tau) \sigma_E(\tau) d\tau \tag{8.7}$$

And the time domain convolution of electric field and electric loss:

$$\Sigma_M(t) = \mu_0 \sum_{i=0}^{q-1} \int_{i\Delta t}^{(i+1)\Delta t} H(t-\tau) \sigma_M(\tau) d\tau \tag{8.8}$$

Next for the piecewise linear approximation of all time dependent fields:

$$X(t) = \sum_{i-0}^{q-1} X^{i+1} - \frac{X^{i+1} - X^i}{\Delta t} (t - i\Delta t) \tag{8.9}$$

For q segments of X, where X can be substituted for E, H.

The recursive accumulators for D, B, Σ_E, Σ_H are defined by subbing 8.9 into any of the expressions with time dependent fields that are being integrated (E, D, Σ_E, Σ_H) and then separating the results out in terms of co-efficients of susceptibility or conductivity.

$$D(t) = \epsilon_0 \epsilon_\infty E(t) + \epsilon_0 \sum_{i=0}^{q-1} \int_{i\Delta t}^{(i+1)\Delta t} E^{i+1} - \frac{E^{i+1} - E^i}{\Delta t}(\tau - i\Delta t)\chi_E^{(1)}(\tau)d\tau \tag{8.10}$$

and B(t):

$$B(t) = \mu_0 \mu_\infty H(t) \quad +$$

$$\mu_0 \sum_{i=0}^{q-1} \int_{i\Delta t}^{(i+1)\Delta t} \left[H^{i+1} - \frac{H^{i+1} - H^i}{\Delta t}(\tau - i\Delta t)\chi_M^{(1)}(\tau) \right] d\tau \quad +$$

$$\mu_0 \sum_{i=0}^{q-1} \int_{i\Delta t}^{(i+1)\Delta t} \int_{i\Delta t}^{(i+1)\Delta t} \left[\left(H^{i+1} - \frac{H^{i+1} - H^i}{\Delta t}(\tau - i\Delta t) \right) \cdot \left(H^{i+1} - \frac{H^{i+1} - H^i}{\Delta t}(t_1 - i\Delta t) \right) \chi_M^{(2)}(\tau, t_1) \right] d\tau dt_1$$

And with the convolution of the field and conductivity:

$$\Sigma_E(t) = \epsilon_0 \sum_{i=0}^{q-1} \int_{i\Delta t}^{(i+1)\Delta t} E^{i+1} - \frac{E^{i+1} - E^i}{\Delta t}(\tau - i\Delta t)\sigma_E(\tau)d\tau \tag{8.11}$$

$$\Sigma_H(t) = \mu_0 \sum_{i=0}^{q-1} \int_{i\Delta t}^{(i+1)\Delta t} H^{i+1} - \frac{H^{i+1} - H^i}{\Delta t}(\tau - i\Delta t)\sigma_H(\tau)d\tau \tag{8.12}$$

Lorentzian form of susceptibility and conductivity:

$$\zeta(t) = Real[\gamma e^{(-\alpha + j\beta t)}]U(t) \tag{8.13}$$

Where $\zeta(t) = \mathscr{F}(\zeta(\omega))$ where $\zeta(\omega)$ is the form $\forall Ł(\omega) \in$ Complex plane, where $Ł(\omega)$ is a general solution to the equation of motion of bodies driven by an incident sinusoidal field and restored by forces with strength proportional to $\frac{1}{r^2}$. CHECK AND MATHIFY

Coefficients of chi, substitution, form of chi, convolution of E field and conductivity are given by: [65]

$$\alpha = \frac{\Gamma}{2} \tag{8.14}$$

$$\beta = \sqrt{\omega_0^2 - \frac{\Gamma^2}{4}} \tag{8.15}$$

$$\gamma = \frac{\omega_p^2}{\beta} \tag{8.16}$$

Where Γ is the full width of the lorentzian curve at half maximum amplitude[66] and U(t) is a step function. CHECK

The recursive accumulators for the linear contributions are defined in general by:

$$\Phi^{l,q} = \pi_0 \sum_{i=0}^{q-1} [X^{i+1} \cdot \theta_0^{l,i} - \left(X^{i+1} - X^i \right) \cdot \theta_1^{l,i}] \tag{8.17}$$

Where $\pi_0 \in \{\epsilon_0, \mu_0\}$ and:

$$\theta_0^{l,i} = \int_{\tau=i\Delta t}^{(i+1)\Delta t} \nu(\tau)d\tau \tag{8.18}$$

$$\theta_1^{l,i} = \frac{1}{\Delta t} \int_{\tau=i\Delta t}^{(i+1)\Delta t} [\tau - i\Delta t]\nu(\tau)d\tau \tag{8.19}$$

Where $\nu(\tau)$ is the operand in a convolution integral that products the field that is being 'slid' over the domain with the (t-τ), time minus dummy parameter argument. For convenience (explain, subbing in of discrete vals interpolation etc) the fields E, H were chosen for sliding functions and χ, σ were chosen to be the operand's being integrated in the recursive accumulators due to the ability to generate a recursion function with the known form of the susceptibility and loss.

For the nonlinear contribution from second harmonic generation:

$$B(t) = \mu_0 \sum_{i=0}^{q-1} \int_{i\Delta t}^{(i+1)\Delta t} \int_{i\Delta t}^{(i+1)\Delta t} \left[(H^{i+1})^2 - (H^{i+1})^2 B + H^{i+1} H^i B - (H^{i+1})^2 A + H^{i+1} H^i A \right.$$
$$\left. + (H^{i+1})^2 AB - 2(H^{i+1} H^i)AB + (H^i)^2 AB \right] \chi_M^{(2)}(t, t_1, \tau)d\tau dt_1$$

Where:

$$A = \frac{(\tau - i\Delta t)}{\Delta t} \tag{8.20}$$

$$B = \frac{(t_1 - i\Delta t)}{\Delta t} \tag{8.21}$$

As H^{i+1} and H^i do not depend on the variables of integration they can be moved outside the integral, and as this is second harmonic generation where two frequencies are degenerate, t1 and tau can be exchanged for just tau. This leads to the recursive accumulator for the second harmonic generation contribution:

$$M^{nl,q} = \mu_0 \sum_{i=0}^{q-1} \left\{ (H^{i+1})^2 \cdot \theta_0^{nl,i} - 2(H^{i+1} H^i - (H^i)^2) \cdot \theta_1^{nl,i} + \left[(H^{i+1})^2 - 2(H^{i+1} H^i) + (H^i)^2 \right] \cdot \theta_2^{nl,i} \right\}$$

Where:

$$\theta_0^{nl,i} = \int_{\tau=i\Delta t}^{(i+1)\Delta t} \chi_M^{(2)}(\tau)d\tau \tag{8.22}$$

Where χ is found via Poutrina equations and transformed to time domain? Integrate just over tau?

$$\theta_1^{nl,i} = \frac{2}{\Delta t} \int_{\tau=i\Delta t}^{(i+1)\Delta t} (\tau - i\Delta t)\chi_M^{(2)}(\tau)d\tau \tag{8.23}$$

$$\theta_2^{nl,i} = \frac{1}{(\Delta t)^2} \int_{\tau=i\Delta t}^{(i+1)\Delta t} (\tau - i\Delta t)^2 \chi_M^{(2)}(\tau)d\tau \tag{8.24}$$

Chapter 9

Next steps

FIX TF/SF EVENTUALLY

Model order reduction (even if I don't go with it write about it)

Chapter 10

MODEL ORDER REDUCTION

10.1 Literature Review

Explain and give history of control theory and MOR. (Observables, Controllables, gramians, discuss krylov subspace methods, expansion of prima style mna Lti utilising cpml and J etc) Treat nonlinear quantities as additional source terms dependent on previous E/H? Or incorporate into expanding set up? PYTHON CONTROL MODULE

Discuss several methods, justify projection choice. TURBOMOR consideration?

Discuss pros and cons of model order reduction in general

LTI form of linear dispersive equations

krylov subspace V vector generation for one sided arnoldi with moment matching to find span size q

eigenvalue pertubation (with or without MOR)

Notes on Jonathan meeting:

Stipend extension requirements:

££££££££££££££6 months extension for money, 6 months deadline need to evidence and argue for stipend extension ££££££££

potential avenues: eigenvalue perturbation and modification of current code update elements

model order reduction:

10.2 Code explanation

10.2.1 MasterController

MasterController acts as a controller for all of the processes involved in the simulation process, evaluation of data, plotting of data, error asssessment, class instantiation, verification etc.

The start of the file contains the definitions for the jitclasses Variables, Params, Convolutional Params and Convolutional Variables, instantiating these classes also initialises the members.

Variables contains objects that change over the course of the simulation.

Params remain constant but will be calculated by Environment Setup based off of basic user input.

CV is the same as variables but specifically related to the cpml

CP is the same as params CONTROLLER FUNCTION; one by one calls functions for simulation, not hooked up to MOR set up. Initialises all vars (may not be necessary if instantiating class each time?) Intergrator, move to separate function. try and move into a numba function? Stop storing Ex History? How to efficiently store values of fields? Probes? Multiple probes + interpolation? 100 probes? Basically read Ex History at Intervals?

Option for no vid output. Instead of video interval, have interval on Ex History storage. Sparsify Histories?

Input section, read in as txt file? Move to another file? Main file?

Results: Requests frequency domain info, then requests calc of reflection coef if reflectCO is true. If analRefCo is true returns analytical ref. Seperate into two functions?

Plotter plots, maybe make more sophisticated otherwise just use built in plotting features. Loopedsim; if Mormode is false, then runs through process for integrator and results. Move mormode false to separate function, loop function if true, with output list. Make output a list for loop and non loop but just 1 val for non loop

Remove fddata things, freq dom data?

If mormode is true, call MORSetup func (new one) instead of running through matrix-Construct funcs.

Expose member fields to inspector.

Consider applying preconditioners For luinvert consider fallback option, pseudo inverse after LU np linalg inv, and scipy splu fail.

conditions no. 5.8 with FOM summer/winter

2e17 with red!!!!

Attempted spectral preconditioner with eig pert and qr decompose it does seem to behave appropriately

time and memory profile each function and write up.

Write up Fdtd equations and mor version.

Shape of projection matrix is wrong.

matrixConstruct:

numba jit function exampleArnoldi, additional qr steps

Initmat ??? Creates A, B source I think this is old redundant code pre-MNA form

coEfFinder: calcs all co efficients for integration steps MOR,

ABuild: Old redundant code pre-MNA

RandFBuild: Constructs R and F matrices for MNA

R and F not built correctly? Upper and Lower triangular?

BasisVector: Initialises Xn

SourceVector: Initialises UnP1A and UnP1B which represent electric and magnetic sources

BGenerator: initialises B

Block builder: Creates K, dE, dH etc for R and F, attempt stabilisation of K here?

TimeIter: Old redundant time stepper

luInvert: Inverts matrices via, splu or LU decomp etc. May consider removing entirely and just solving via solvers? If solvers don't work, try adding pseudo inverse as a last resort.

smooth: Takes in signal and convolves with smoothing window

solnDenecker: Contains prep for time stepping and timeStepping, needs to be refactored. Initialises XnP1

sets k value, just randomly input by user, maybe find method for choosing appropriate? Calls creates 'summer' and 'winter' with (R+F) and (R-F). Checks von Neumann stability of summer and winter creates M which is fed into Arnoldi Calls Arnoldi which seems to create feasible projection matrix

Avoid inverse, just try solving, use preconditioner in solver Attempts sprim, preserve structure... Check structure of matrices?

Inverse AA in order to have it act as preconditioner?

If not jacobian preconditioner. But use jacobian (diag of H)

BASEFDTD:

sourceGen 1 and 2 debug sources

fieldInit: initialise all field quantities, redundant with class instantiation? asserts lots of properties, refactor field init into master controller file as check for user inputs?

Smoothturnon: Manages smooth turn on of source for TF/SF method, but TF/SF isn't working, so try cpml left edge and just normal pulse? Just Ex source? CPML will absorb reverse wavelet and then reflected wavelet from right PEC/dielectric edge will be only one considered.

EmptySpaceCalc:

Calculates params for empty space, probably don't need to do this everytime as const.

FUTURE RE-DERIVATION OF singular val perturbation = Keeping R red positive definite

step 1: Reconstruct R: such that R+F and R-F upper and lower diagonal? use Schur Complement equations to derive conditions for positive definiteness, i.e. new singular value bound, find form using schur complement which isolates operator for perturbing as oppose to value matrix.

interesting proof of structure preservation, grab vs direct reduce.

Summer red is too badly conditioned for solve, blows up.

lgmres next More preconditioners.

Qr factorisation?

Attempting spilu preconditioner in gmres for time stepping.

System needs to detect when to use nonlinear solver.

lgrmes with previous soln as approximate?

Try without singular

CPML REGION CHECK OPTIONAL SPLU MAGOO CSC NEEDED

REPORT JITCLASS, OUTPUTS TO FILE SO CONSOLE LESS VERBOSE AND INFO MORE ORGANISED.

10.3 FDTD in matrix form

MAXWELL EQNS CONTINUOUS TO DISCRETE TO MOR VERSION WITH BC'S AND FULL EXPLANATION OF CODE REQUIREMENTS.

Material equations in time domain cont in time CONT then DISC form nonlinearity in case of single split ring resonator stems from magnetic susceptibility.

$$\nabla \times H(t) = \frac{\partial D}{\partial t} + \sigma_E \star E(t) \tag{10.1}$$

$$\nabla \times E(t) = -\frac{\partial B}{\partial t} + \sigma_M \star E(t) \tag{10.2}$$

Where D is:

$$D(t) = \epsilon_0 \epsilon_\infty E(t) + \epsilon_0 \int_0^T E(t-\tau)\chi_E^{(1)}(\tau)d\tau \tag{10.3}$$

And B is:

$$B(t) = \mu_0 \mu_\infty H(t) + \mu_0 \int_0^T H(t-\tau)\chi_M^{(1)}(\tau)d\tau \tag{10.4}$$

$$+\mu_0 \int_0^T \int_0^T H(t-\tau)H(t-t_1)\chi_M^{(2)}(\tau,t_1)d\tau dt_1$$

We also have:

$$\nabla \cdot B = 0 \tag{10.5}$$

$$\nabla \cdot D = \rho_{free} \tag{10.6}$$

PEC boundary condition (simply enforce boundary terms to be zero)
CPML boundary conditions:
In the frequency domain, create a stretched co-ordinate space using:

$$j\omega\epsilon E_x + \sigma E_x = \frac{\partial}{sy\partial y}H_z - \frac{\partial}{sz\partial z}H_y \tag{10.7}$$

Where s_i is:

$$s_i = 1 + \frac{\sigma_i}{j\omega\epsilon_0} \tag{10.8}$$

For i = x, y, z. ref Berenger PML
Then transform to time domain and using the fact that multiplication in the frequency domain is congruent to convolution in the time domain:

$$\frac{\epsilon\partial}{\partial t}E_x + \sigma E_x = \tilde{s}_y(t) * \frac{\partial}{\partial y}H_z - \tilde{s}_z(t) * \frac{\partial}{\partial z}H_y \tag{10.9}$$

Where the * signifies a convolution operation and $\tilde{s}_i$ refers to the inverse laplace transform of $\frac{1}{s_i}$

To incorporate this entire model, the time continuous system can be converted to a time discrete one whereby the PDE can be modelled iteratively in a leap-frog pattern, with a yee grid stencil. A nonlinear auxiliary differential equation can be used to model the nonlinear dispersion. The yee grid update equations can then be utilised in matrix format to enable model order reduction techniques and also additional perturbation based stabilisation extensions.

10.3.1 Discrete version of free space update equations in yee grid

The free space update equations in time discrete form with leap-frog Yee grid style iterations are written as:

$$Hy_{k+\frac{1}{2}}^{n+\frac{1}{2}} = Hy_{k+\frac{1}{2}}^{n-\frac{1}{2}} + \frac{\Delta_t}{\mu \Delta_x}(Ex_{k+1}^n - Ex_k^n) \tag{10.10}$$

$$Ex_k^{n+1} = Ex_k^n + \frac{\Delta_t}{\epsilon \Delta_x}(Hy_{k+\frac{1}{2}}^{n+\frac{1}{2}} - Hy_{k-\frac{1}{2}}^{n+\frac{1}{2}}) \tag{10.11}$$

A simple additive source can be incorporated by adding a term to the electric (or magnetic) update equations, from a vector of snapshots of the electric (magnetic field) values over time. For example, a simple sine source would be extracted from a vector of:

$$sin(2\pi f t_i) \tag{10.12}$$

Where f is frequency in Hz and t_i is each time step (t0 + $N_{timesteps}$ * time interval), the value for each time step is stored in a vector and elements of this vector are added to the update equations by iterating the t_i vector over each time step of the simulation. If a source is added to the update equations this will act as a soft source, as oppose to a hard source which forces the source location of the simulation grid to take on a given value. Hard sources will also act like perfect electric(magnetic) conductor boundary conditions as they will reflect incident waves. To enforce perfect electric (magnetic) conductor boundary conditions at any point within the simulation domain, the node is simply set as zero. A simple implementation for the edge of the domain is to add zero valued nodes onto the edge of the array containing the electric (magnetic) field values. In one dimensional simulations absorbing boundary conditions can be employed to absorb waves (act as though waves are propagating off beyond simulation domain) by setting the edge nodes equal to nodes the inverse of the courant number ($\frac{1}{S_c}$) distant. In higher dimensional sims though this does not work, so perfectly matched layers can be used. Perfectly matched layers act like a conductive layer which attenuates the wave. In order to avoid reflection at the PML interface, Berenger proposed the split field PML whereby the perpendicular components of an incident wave are handled separately. A further improvement to the PML is the CPML or convolutional perfectly matched layer introduced by Gedney and Roden. This method introduces complex co-ordinate stretching to the simulation domain which attenuates the wave without reflections at the interface, regardless of the domain material. CPML in continuous formulism is seen above in 10.9, in discrete form the CPML update equations utilise the known impulse of the CPML in the frequency domain, to transform the CPML to time domain and make it applicable to finite difference time domain simulations without the requirement of expensive Fourier transform operations at each time step. For the time domain discrete form, the stretching variable S_i proposed by Kuzuoglu and Mittra can be used:

$$S_i = \kappa_i + \frac{\sigma_i}{\alpha_i + j\omega\epsilon_0} \tag{10.13}$$

Where i = x,y,z.

Via Laplace transform theory it can be shown that the inverse of S_i, $S_i^{-1} = \tilde{S}_i$ has the following impulse response that can be utilised to derive a time domain formulism for the CPML:

$$\tilde{S}_i = \frac{\delta(t)}{\kappa_i} - \frac{\sigma_i}{\epsilon_0 \kappa_i^2} e^{-((\frac{\sigma_i}{\epsilon_0 \kappa_i}) + (\frac{\alpha_i}{\epsilon_0}))} u(t) \tag{10.14}$$

$$= \frac{\delta(t)}{\kappa_i} + \zeta_i(t) \tag{10.15}$$

Where α_i is the complex shifting parameter, u(t) is a step function, σ_i is the CPML conductivity term and κ_i is a real positive term. All the CPML constitutive terms are scaled via polynomials dependent on grid distance and independent of frequency.

Lead into ADE linear CPML discrete

discrete versions with O(2) central diff integrator for free space. ADE linear dispersive CPML Nonlinear ADE dispersive Nonlinear (resonance tuning)

then matrix form then MNA matrix form MOR with PRIMA and SPRIM then singular val perturbation then theoretical expansion of MOR to incorporate linear dispersion and CPML

10.4   Free space time continuous to time discrete

Firstly, convert current system into a matrix across space not time, in the form MNA: CXn+1= -Gxn + Bun+1

Verify accuracy of model H2/Hinf norm checks, early in run?

10.5   Find transfer function in laplace domain

the transfer function of an LTI is given, use to find the krylov subspaces for two sided arnoldi.

10.6   Moment matching

Match moments to find a good value for q size of krylov subspaces?

10.7   Projection of X onto Xred

Write down MORTEST steps

Move MORTest into actual code. Polyfit seems to capture harmonic properties. Re-derive MNA to expand.

Work to write about: FFT to check harmonics, find H2 norm and H inf norm to check FOM vs ROM.

DEFENSIVE PROGRAMMING

Bibliography

[1] A. S. Gilmour Jr, "Klystrons, Traveling Wave Tubes, Magnetrons, Cross Field Amplifiers and Gyrotrons", Artech House Publishing, Textbook, 2011

[2] J. R. Pierce, "Theory of the Beam-Type Traveling-Wave Tube", Proceedings of the I.R.E, 1947

[3] R. Kompfner, "The Traveling-Wave Tube as Amplifier at Microwaves", PROCEEDINGS OF THE I.R.E. February 1944

[4] L. R. Barnett et al, "Theory and experiment of a 94 GHz gyrotron traveling-wave amplifier", Physics of Plasmas, Article, 2004

[5] J. R. Sirigiri et al, "A Novel Wideband Gyroton traveling wave amplifier ", PhD thesis, Massachusetts Institute of Technology, 2002

[6] R. M. Walser, "Electromagnetic Metamaterials.", Proceedings of SPIE - The International Society for Optical Engineering 4467 July 2001

[7] A. Mahmoud, "DESIGN STUDY OF THE 455 GHz, 1.027 kW SECOND HARMONIC GYROTRON OSCILLATOR", Lambert Academic Publishing, Textbook, 2013

[8] G. Faillon, "Vacuum Electronics, Components and Devices", Chapter 1, 2008

[9] G. S. Nusinovich et al, "Gyro at 50: Historical Review", J infrared milli Terahz waves 2014, invited review article

[10] M. Thumm, "HISTORICAL GERMAN CONTRIBUTIONS TO PHYSICS AND APPLICATIONS OF ELECTROMAGNETIC OSCILLATIONS AND WAVES", www.radarworld.org/history.pdf as seen 15/06/2018

[11] G. Caryotakis,"The Klystron: A Microwave Source of Surprising Range and Endurance" SLAC–PUB–7731 April 1998 - Rev

[12] Website author unknown, "Travelling tubes on Tutorialspoint.", https://www.tutorialspoint.com/microwave_engineering/ microwave_engineering_travelling_wave_tube.htm, as seen on 15/06/2018

[13] Y. S. Tan, R. Seviour, "Wave Energy Amplification in a Metamaterial based Traveling Wave Structure", EPL (Europhysics Letters), Volume 87, Number 3, 2009

[14] R. Seviour, "Introduction and Overview of the Book - Rebecca Seviour chapter lead" John Q Public: The public book, chapter 1, 2017

[15] 3rd Baron Rayleigh, "On the influence of obstacles arranged in rectan- gular order upon the properties of a medium", Phil. Mag, 5 (34), 481, 1892

[16] J. C. Bose, "On the rotation of plane of polarisation of electric waves by a twisted structure.", Proc R. Soc. Lon., 63, 146, 1898

[17] W. E. Kock, "Metallic Delay Lenses.", Bell System Technical J, 27, 58, 1948

[18] J. B. Pendry, A. J. Holden, W. J. Stewart, I. Youngs, "Extremely Low Frequency Plasmons in Metallic Mesostructures", Physical review letters, VOLUME 76, NUMBER 25, 1996

[19] Q. Wu, F. Meng, M. Wu, J. Wu, L. Li, "Research on the Negative Permittivity Effect of the Thin Wires Array in Left-Handed Material by Transmission Line Theory", Progress In Electromagnetics Research Symposium China, 2005

[20] V. G. Veselago, "The electrodynamics of substances with simultaneously negative values of ϵ and μ. Usp. Fiz. Nauk, 92, 517-526, 1967

[21] X. Tang et al, "Dual Band Metamaterial Cherenkov Oscillator With a Waveguide Coupler", IEEE TRANSACTIONS ON ELECTRON DEVICES, VOL. 64, NO. 5, MAY 2017

[22] S.A. Schelkunoff, H. T. Friis, "Antennas: Theory and Practise", John Wiley and sons, 1952

[23] C. Sabah, S. Uckun, "Electromagnetic wave propagation through frequency-dispersive and lossy double-negative slab", OPTO-ELECTRONICS REVIEW 15(3), 133–143, 2007

[24] A. Alu, N. Engheta, "Pairing an Epsilon-Negative Slab With a MuNegative Slab: Resonance, Tunneling and Transparency" University of Pennsylvania, Departmental papers, Department of Electrical and systems Engineering, 2003.

[25] TLY-5A data sheet, provided by 4Taconic, http://www.4taconic.com, last seen 28/08/18

[26] FR4 data sheet, provided by rogerscorp, http://www.rogerscorp.com/documents/2359/acm/articles/, last seen 28/08/18, published 1996.

[27] J. Z. Sanborn, C. Hellings, T. D. Donnelly, "Breakdown of the slowly-varying-amplitude approximation: generation of backward-traveling, second-harmonic light", Department of Physics, Harvey Mudd College, Claremont, California 91711, 2002

[28] M. Azari et al, "Coupled equations of electromagnetic waves in nonlin- ear metamaterial waveguides", Applied Optics, Vol. 55, No. 31, 2016

[29] I. V. Shadrivov, et al, "Colloquium: non-linear metamaterials", Review of Modern Physics, 2014

[30] O. Sydoruk, "Tailoring the properties of metamaterials for linear and non-linear applications", PhD Thesis, University Osnabruck, 2007

[31] D. R. Smith, et al, *"Electromagnetic parameter retrieval from inhomogeneous metamaterials"*. Phys. Rev. E, 71 (036617), 2005

[32] A. Rose, "Theory and Design of non-linear Metamaterials", PhD thesis Duke University, 2013

[33] E Poutrina et al, "Analysis of non-linear Electromagnetic Metamaterials", New J. Phys. 12 093010, 2010

[34] J.D.Baena et al, "Equivalent-circuit models for split-ring resonators and complementary split-ring resonators coupled to planar transmission lines", IEEE Transactions on Microwave Theory and Techniques (Volume: 53, Issue: 4, April 2005)

[35] G. New "Introduction to non-linear optics", Cambridge Press, 2012

[36] S. Gold, G. S. Nusinovich, "Review of higher-power microwave source research", Review of Scientific Instruments 68(11):3945-3974, November 1997

[37] R A Lewis "A review of terahertz sources" J. Phys. D: Appl. Phys. 47 374001, 2014

[38] M. Field et al, "Development of a 100-W 200-GHz High Bandwidth mm-Wave Amplifier", IEEE TRANSACTIONS ON ELECTRON DEVICES, VOL. 65, NO. 6, JUNE 2018

[39] Z. Zaojin, et al, "Design and optimization of a W-band extended interaction klystron amplifier", IEEE International Vacuum Electronics Conference (IVEC), 2015

[40] C. Sirtori, "Applied physics: Bridge for the terahertz gap", Nature volume 417, pages 132–133 May 2002

[41] R. Barker, E, Schamiloglu, "High-Power Microwave Sources and Technologies." IEEE press series on electromagnetic waves, 2001.

[42] S. Larouche, D. R. Smith, "A retrieval method for non-linear metamaterials", Optics Communications 283 1621–1627, 2010

[43] W.H.Louisell, "Coupled mode and parametric electronics", John Wiley and sons, 1960.

[44] P. Sprangle, V. Granatstein, A. Drobot. "THE ELECTRON CYCLOTRON MASER INSTABILITY." Journal de Physique Colloques, 1977,

[45] Yashvir Kalkal, et al, "Analysis of Čerenkov free-electron lasers" PHYSICAL REVIEW SPECIAL TOPICS - ACCELERATORS AND BEAMS 18, 030707 (2015)

[46] W. Main et al, "High-Power Dielectric Cherenkov Maser Oscillator Experiments", IEEE TRANSACTIONS ON PLASMA SCIENCE. VOL. 18. NO. 3. JUNE 1990

[47] F. He et al, "Linear Theory of Double Slot Coupled Cavity Slow Wave Structure in TWT", Key Laboratory of High Power Microwave Sources and Technologies, Institute of Electronics, Chinese Academy of Sciences, date unknown.

[48] S. A. Kishko et al, "Low-Voltage Cyclotron Resonance Maser", IEEE TRANSACTIONS ON PLASMA SCIENCE, VOL. 41, NO. 9, SEPTEMBER 2013

[49] Q. F. LI, et al, "Theory of Gyrotron Traveling-Wave Amplifiers", IEEE TRANSACTIONS ON MICROWAVE THEORY AND TECHNIQUES, VOL. MTT-34, NO, 10, OCTOBER 1986

[50] A. M. Ferendeci, et al, "RECTANGULAR CAVITY HIGH HARMONIC GYROTRON AMPLIFIER ", NASA Lewis Research Center, date unknown.

[51] Q. S. Wang, et al, "High-Power Harmonic Gyro-TWT's-Part 11: non-linear Theory and Design ", IEEE TRANSACTIONS ON PLASMA SCIENCE, VOL. 20, NO. 3, JUNE 1992

[52] S. V. Samsonov, et al, "Ka-Band Gyrotron Traveling-Wave Tubes With the Highest Continuous-Wave and Average Power ", IEEE TRANSACTIONS ON ELECTRON DEVICES, VOL. 61, NO. 12, DECEMBER 2014

[53] D. Shiffler et al, "A Cerenkov like maser based on metamaterial structure", IEEE TRANSACTIONS ON PLASMA SCIENCE, VOL. 38, NO. 6, JUNE 2010

[54] M. A. Shapiro et al, "Active Negative Index Metamaterial Powered by an Electron Beam", Physics optics, 2012

[55] O. V. Sinitsyn, et al, "non-linear Theory of the Gyro-TWT: Comparison of Analytical Method and Numerical Code Data for the NRL Gyro-TWT", IEEE TRANSACTIONS ON PLASMA SCIENCE, VOL. 30, NO. 3, JUNE 2002

[56] C. Rivera, "Effects of electrostatic force on piezoelectric materials under high electric field: Impact on GaN-based nanoscale structures ", Ingeniería y Servicios Aeroespaciales S.A., Paseo Pintor Rosales 34, 28008 Madrid, unknown date.

[57] D. Huang, PhD thesis Duke University, "Development of Analog non-linear Materials Using Varactor Loaded Split-ring Resonator Metamaterials ", 2013

[58] Y. Y. Lau, et al, "A note of Gyrotron travelling wave tubes using rectangular waveguides", IEEE TRANSACTIONS ON ELECTRON DEVICES, VOL. ED-30, NO. 8, AUGUST 1983

[59] K. C. Leou et al, "Dielectric-Loaded Wideband Gyro-TWT", IEEE TRANSACTIONS ON PLASMA SCIENCE, VOL. 20, NO. 3, JUNE 1992

[60] S. Larouche et al, "Retrieval of all effective susceptibilities in non-linear metamaterials",physics.optics, 2017

[61] A. M. Ferendecci et al, "Theory of High-Harmonic Rectangular Gyrotron for TE_{MN} Modes ", IEEE TRANSACTIONS ON ELECTRON DEVICES, VOL. ED-31, NO. 9, SEPTEMBER 1984

[62] P. H. Vartanian, et al, "Propagation in Dielectric Slab Loaded Rectangular Waveguide", IRE TRANSACTIONS ON MICROWAVE THEORY AND TECHNIQUES, 1958

[63] Z. Wang, et al, "Second-Harmonic Generation and Spectrum Modulation by Active non-linear Metamaterial ", The Electromagnetic Academy at Zhejiang University, unknown date.

[64] T. M. Antonsen, et al, "Traveling-Wave Tube Devices with non-linear Dielectric Elements", IEEE TRANSACTIONS ON PLASMA SCIENCE, VOL. 26, NO. 3, JUNE 1998

[65] Ayşegül P. et al, "FDTD-Based Metamaterial (MTM) Modeling and Simulation", EEE Antennas and Propagation Magazine, Vol. 56, No. 5, October 2014

[66] Maxwell J. Mageto et al, "The Lorentz Oscillator Model Simulation Illustrating a Broad Maximum in the Bulk Reflectance for Frequencies Just Above the Resonance Frequency", The African Review of Physics (2012)

Appendix A

Progression monitoring 1 and verification examples

Appendix B

Gantt Chart